Laser surface processing with controlled nitrogen-argon concentration levels for regulated surface life time

M. Ahmed Obeidi, E. McCarthy, D. Brabazon

Advanced Processing Technology Research Centre,

School of Mechanical & Manufacturing Engineering,

Dublin City University, Dublin 9, Ireland

Abstract

Laser surface modification can be used to enhance the mechanical properties of a material, such as hardness, toughness, fatigue strength, and corrosion resistance. Surface nitriding is a widely used thermochemical method of surface modification, in which nitrogen is introduced into a metal or other material at an elevated temperature within a furnace. It is used on parts where there is a need for increased wear resistance, corrosion resistance, fatigue life, and hardness. Laser nitriding is a novel method of nitriding where the surface is heated locally by a laser, either in an atmosphere of nitrogen or with a jet of nitrogen delivered to the laser heated site. It combines the benefits of laser modification with those of nitriding. Recent work on high toughness tool steel samples has shown promising results due to the increased nitrogen gas impingement onto the laser heated region. Increased surface activity and nitrogen adsorption was achieved which resulted in a deeper and harder surface compared to conventional hardening methods. In this work, the effects of the laser power, pulse repetition frequency, and overlap percentage on laser surface treatment of 316L SST steel samples with an argon-nitrogen jet will be presented. Resulting microstructure, phase type, microhardness, and wear resistance are presented.

1 INTRODUCTION

Laser surface modification is a beneficial processing method that can be used to enhance the mechanical properties of a material, such as hardness [1], wear resistance [2], fatigue strength [3], and corrosion resistance [4]. Surface nitriding is a thermochemical method of surface modification, in which nitrogen is incorporated into a metal or other material, at an elevated temperature. It can increase wear resistance, corrosion resistance, fatigue life, and hardness of parts [5]. In its most basic form, gas nitriding, it is performed by heat-treating the material in a pure nitrogen, or often ammonia [5], atmosphere. The process requires a long exposure time, up to 75 hr. The advantages of conventional furnace gas nitriding include the improved hardness, sliding wear resistance, and corrosion resistance, that it can be performed below the phase transformation temperature, that it requires no further processing such as quenching (which could introduce warping or cracks), and that the modified layer does not alter the dimensions of the part. The main disadvantage of conventional furnace gas nitriding is its processing time. Other common types of nitriding are plasma nitriding and ion-beam nitriding, which can decrease the time and temperature needed compared to gas nitriding [6].

Laser nitriding is a novel method which combines laser surface modification with nitriding. In laser nitriding, a laser is used as the heat source, focused on the surface of the material to locally heat the surface, either in an atmosphere of nitrogen or with a jet of nitrogen delivered to the laser heated site. The technique was first reported by Katayama et. al. in 1983 [7], and has been successfully applied to many different materials and alloys, such as iron, carbon steel, stainless steel, aluminium, and titanium [5][8][9][10]. Laser nitriding compares favourably to other nitriding methods, achieving comparable hardnesses and treatment depths to gas nitriding in the shortest treatment time compared to gas, plasma, or ion-beam methods [6].

Laser surface modification alone can improve the hardness and wear resistance of metal surfaces. Aqida et. al. improved the surface hardness of AISI H13 tool steel from ~300 HV to up to 1017 HV using a 1.5 kW CO_2 laser at powers of 825-1050 W, with a jet of argon delivered in line with the beam [4]. Majumdar et. al. compared the results obtained using a jet of argon, nitrogen, or a 50/50 mix of the two gases, with a 2 kW CO_2 laser on the surface of SAE 52100 tool steel [1]. The authors found increases of microhardness ranging from ~100-200 HV for the argon jet, up to 650 HV for the nitrogen jet, and up to 700 HV for the 50/50 mixture. The wear resistance was found to improve with the hardness.

Using 100% N_2 gas may result in surface cracks and brittleness. Sun et. al. and Mridha et. al. found the formation of the surface macro/micro-cracks in a Ti-6Al-4V alloy laser nitrided with 100% N_2, due to the high cooling rates [11,12]. Sun et. al. reported that optimising the main laser processing parameters could reduce the residual stresses in the altered layer, and thus reduce the occurrence of surface cracks [11]. Alternatively, the application of diluted nitrogen, typically diluted with argon, can reduce cracks. However, this may also reduce the hardness achieved. Several researchers have used different ratios of argon-nitrogen gas mixtures [1,12–18]. Argon gas is typically chosen as the diluting gas because it decreases the surface tension of the molten material melted by the laser, allowing deeper penetration of the nitrogen in the mixture [19].

Nitriding to improve the properties of steel has possible applications in making rolling fatigue resistant gears [20], cut blades [21], bipolar plates in proton exchange membrane fuel cells [22], and biomedical applications such as surgical instruments [23]. In this work, the effect of laser processing 316L stainless steel using an argon-nitrogen mix jet, with varied laser powers (P), pulse repetition frequencies (PRF), and percentage overlap (OV%) was investigated. The resulting samples were characterised in terms of their microstructure, phase types, microhardness, and wear.

2 Materials and methods

In this work, a computerised numerical control (CNC) CO_2 laser machine Rofin DC-015 of 1.5 kW maximum average power and a laser beam focus diameter of 0.2 mm was used. Gas could be delivered in line with the beam, using either pure argon or a mixture of 20% argon and 80% nitrogen at 0.3 mPa. A higher pressure jet may cause spreading and loss of molten material, the pressure of 0.3 mPa was found to give good results in terms of hardness with acceptably low physical material impingement. The materials used were 316L stainless steel cylindrical pins of 10 mm diameter. The cylindrical samples were processed by rotating the pin while scanning the laser linearly, to scan the laser spot over the surface of the pin in a spiral. The rotational and linear speeds could be controlled to adjust the overlap of subsequent laser spots, as well as the overlap of each line of the spiral with the previous line [24].

The laser parameters were applied according to the Box-Behnken experiment design shown in Table 1, varying the laser power (P), pulse repetition frequency (PRF), and percentage overlap (OV%) to produce 17 samples. In each case, the percentage overlap value was applied both for the overlap between consecutive laser spots and the overlap between consecutive laser tracks. Negative values of overlap correspond to the laser spots and tracks being spaced apart by a given percentage of the spotsize. The energy density threshold for melting for 316L SST is in the range of 22-25 J/mm^2. The parameters in the DoE were chosen to be slightly above the melting threshold, to give minimal material loss via ablation. The laser pulse durations corresponding to the PRF values used are 5, 2.5, and 1.67 ms for 100, 200, and 300 Hz, respectively. One parameter set was reproduced on flat stainless steel, converting the rotational speed to linear speed and rastering back and forth in lines, using argon or nitrogen, to allow for pin-on-disc wear testing.

Table 1 Parameters and levels used for the Box-Behnken design of experiment.

	Level 1	Level 2	Level 3
Power (W)	300	400	500
PRF (Hz)	100	200	300
Overlap (%)	-20	0	20

Table 2 Mass percentages for the chemical composition of the cylindrical 316L stainless steel samples.

C	Mn	Cr	Ni	Si	P	S	Mo	N	Cu	Co	Fe
0.018	1.77	17	11.1	0.34	0.033	0.029	2.06	0.029	0.34	0.15	Bal

After processing, the microhardness, microstructure, and wear resistance were characterised. To observe the microstructure, samples were cross-sectioned, then ground and polished using a Buehler Motopol 2000. Successive grades of SiC paper of 400, 600, 800, and 1200 were applied under water flow. Final polishing was then performed using a Textmet cloth with succesive diamond and alumina suspensions of 9, 6, 3, and 0.05 μm particle size. The polished surfaces were then etched with a 5% nital etchant, made up of 95% nitric acid and 5% ethanol, by applying to the surface for 3-5 seconds with a cotton swab before rinsing. The etched surfaces were then observed by Carl Zeiss LS15 scanning electron microscope. The microhardness was measured in terms of the Vickers microhardness using a Leitz mini-load tester. The hardness indents were taken according to ASTM E18-15 with the average of five indents at specified distances from the surface recorded. A distance of five times the indent surface displacement was also used between indents in order to ensure no interference from possible strain hardening effects from previous indents. The wear was tested by the ASTM G-99 pin-on-disc standard, using a 2.5 kg load, a rotational speed of 200 RPM, a track radius of 4 mm, and a testing time of 120 minutes. The pins used were tungsten carbide punch pins from LinkTooling, with a hardness of 775-834 HV.

3 Results and discussion

3.1 Altered surface hardness

The average hardness of the untreated stainless steel cylindrical samples was found to be 250-280 HV. The hardness after laser processing with the argon-nitrogen gas mixture was found to have increased significantly for a number of samples. The hardness recorded for the Box-Behnken samples laser processed with 20%Ar-80%Ni or with 100% Ar can be seen in Table 3. The highest value, of 590 HV found for sample 6 treated with the argon-nitrogen mix, is over double the untreated hardness. The average hardness for the five replicates at 400 W, 200 Hz, and 0% overlap with 20%Ar-80%Ni is 333 HV, with a 95% confidence interval of 16 HV. The improvement in the hardness had depths of up to 900 μm. In Figure 1, a plot of hardness vs depth for sample 1 and sample 6 of the set processed with 20%Ar-80%Ni, the samples with the highest hardness at the surface, is shown. The hardness decreases with depth, with sample 6 reaching the initial bulk hardness at ~900 μm below the surface, and remaining >500 HV for over 400 μm. These depths are significantly above those noted for plasma nitriding of 316L SST, where Biehler et. al. for example measured nitriding depths of ≤ 7.2 μm for plasma nitriding with 300 Pa pressure [25]. However, these authors achieved surface hardness of up to 1,662 HV.

Table 3 Laser parameters and resulting microhardness for the laser processed SST pin samples.

Sample	Power (W)	PRF (Hz)	OV%	20%Ar-80%Ni Microhardness (HV)	100%Ar Microhardness (HV)
1	300	200	-20	549	342
2	400	200	0	301	304
3	400	300	-20	446	338
4	400	200	0	342	304
5	500	200	-20	363	324
6	400	300	20	590	347
7	500	300	0	331	346
8	400	200	0	339	304
9	400	200	0	345	304
10	400	100	20	307	313
11	400	100	-20	462	313
12	300	300	0	300	344
13	300	200	20	326	343
14	500	100	0	315	343
15	500	200	20	286	243
16	300	100	0	310	313
17	400	200	0	338	304

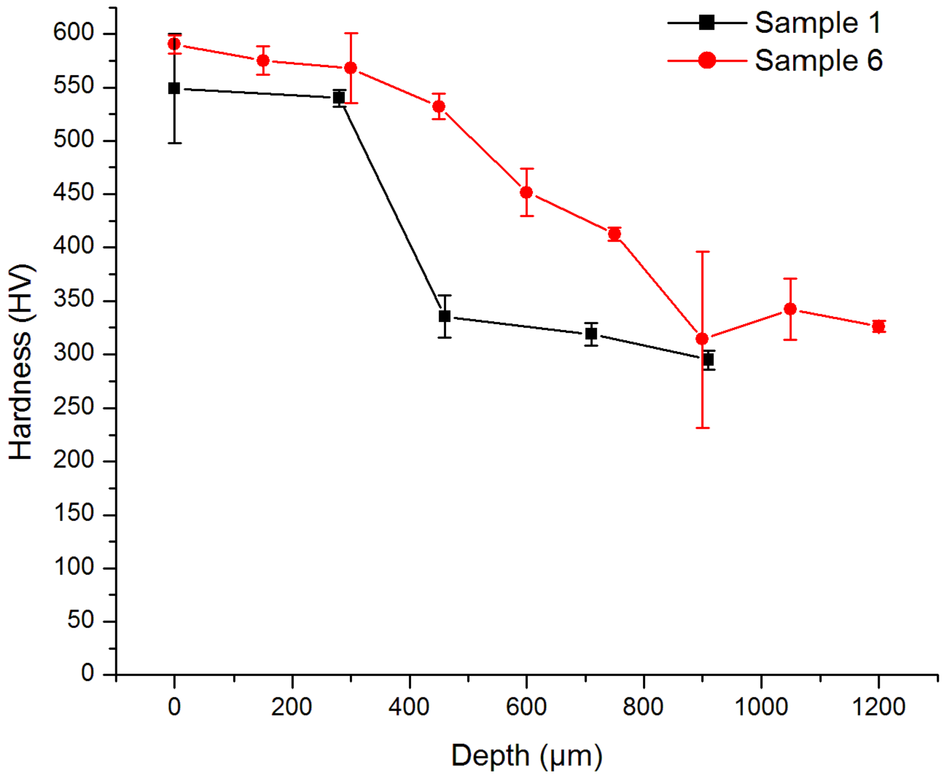

Figure 1 Plot of surface microhardness vs. depth from the surface for sample 1 and sample 6.

The data from Table 3 is shown as response surface graphs in Figure 2 to illustrate the effect of the laser processing parameters on the resulting micro-hardness of the 316L stainless steel cylindrical samples. Figure Figure 2 (b) indicates a strong direct proportionality between the PRF and the resulting hardness at the surface. This agrees with trends reported in the literature [5]. This relationship can be explained by the higher PRF leading to a shorter residence time and therefore faster solidification which is known to result in a harder surface material. Achieving the same overlap with a higher PRF requires using higher linear and rotational speeds, and at higher speeds the laser will be resident on a given area for less time. This shorter residence will lead to higher cooling rates, and higher cooling rates are known to give increased hardnesses [26]. The hardness is highest at the middle power level. The increased heating at higher powers produces more melting, and slower cooling and resolidification, of the metal at the surface. The heating can act as annealing and allow relaxation of the grains, giving lower hardness. Conversely, low power may lead to insufficient heating/melting.

However, Figure Figure 2 (a), in which the laser tracks are spaced apart did not show a strong proportionality with PRF. For this negative overlap, the power is the significant factor, with an inverse proportionality with the hardness. Again, high power may lead to slower re-solidification of the molten material, leading to lower harnesses.

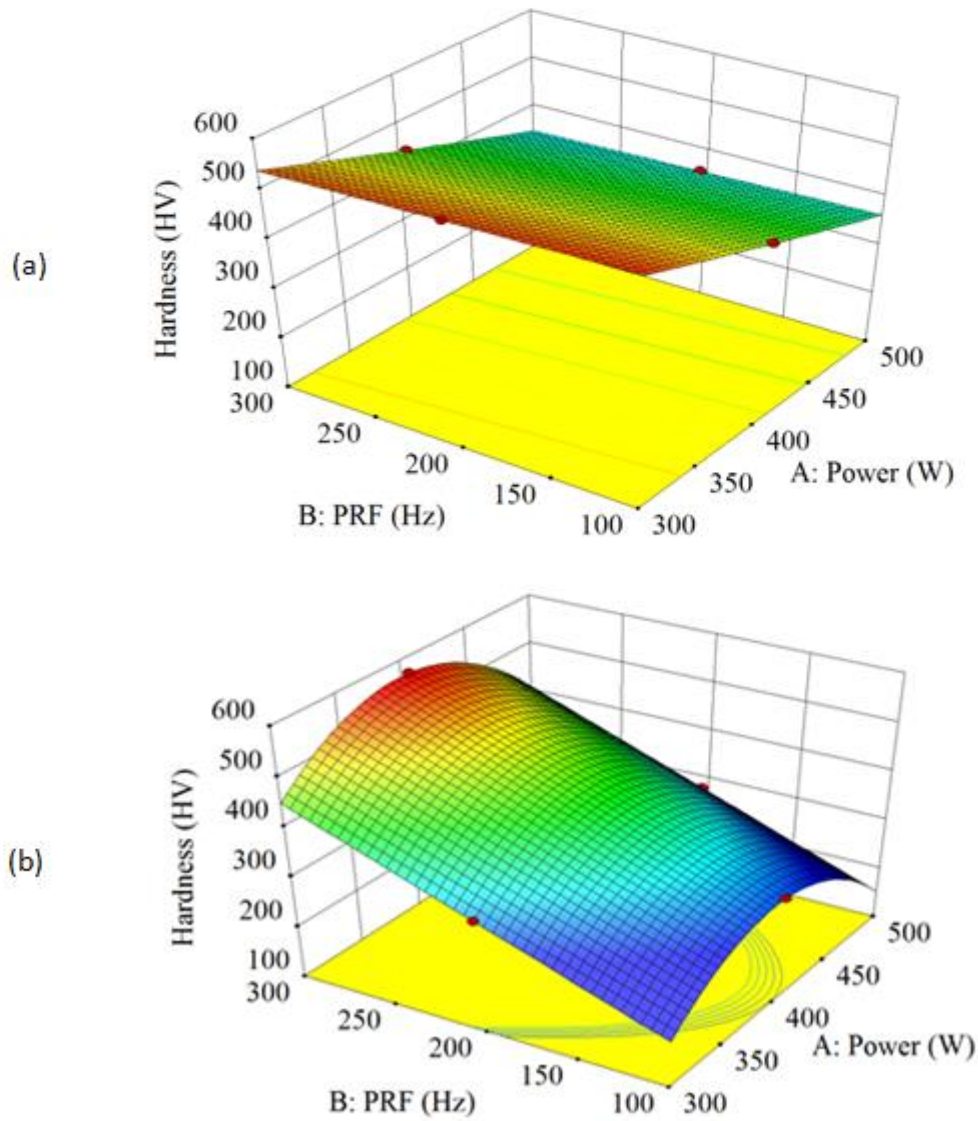

Figure 2 3D RSM plots of the hardness response for the stainless steel

pins processed with 20%Ar-80%Ni with (a) -20% and (b) +20% overlap.

The correlation is also shown in the perturbation plot, see Figure 3, which is taken at 400 W, 200 Hz, and 20% overlap. In a perturbation plot, a single parameter in the RSM model (shown in FigureFigure 2) is varied, while keeping the other parameters constant, to determine the effect of all factors at a given point in the DoE. The x-axis is given in coded units, where -1 indicates a level lower and 1 indicates a level higher. The plot shows that the percentage overlap also has a strong, direct proportionality on the micro-hardness, at this point. It can also be concluded that lower pulse energy and fluence gives higher surface hardness. This conclusion was also reached by Schaaf [5]. Figure 4 shows the measured values against the modelled values (with the equation for the model included), from the RSM model seen in Figure 2, for the box Behnken experimental design, with good agreement between the model and the experimental data.

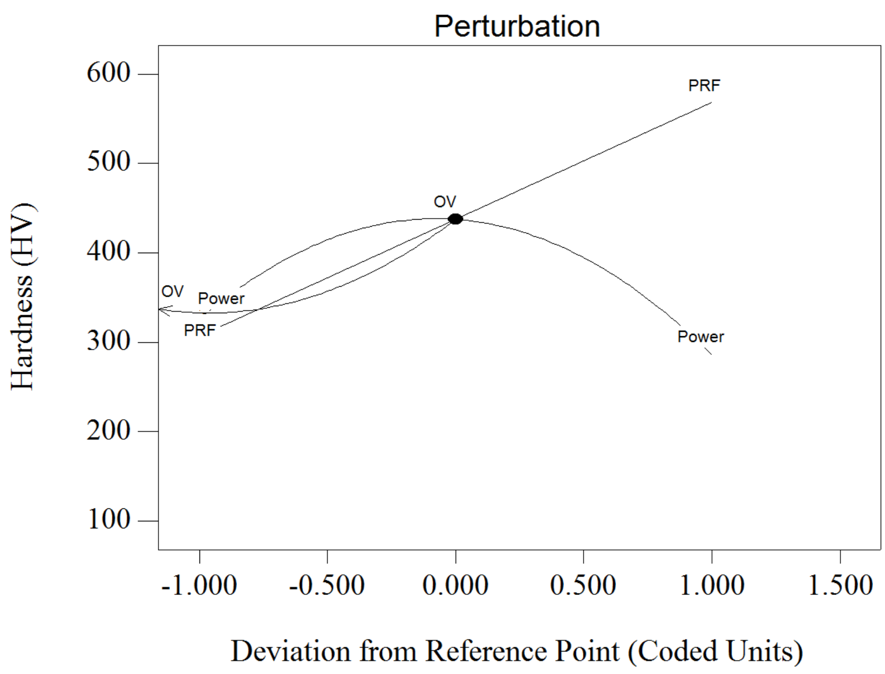

Figure 3 Perturbation plot of the processing parameters and resulting hardness

taken at 400 W, 200 Hz, and 20% overlap, using 20%Ar-80%Ni.

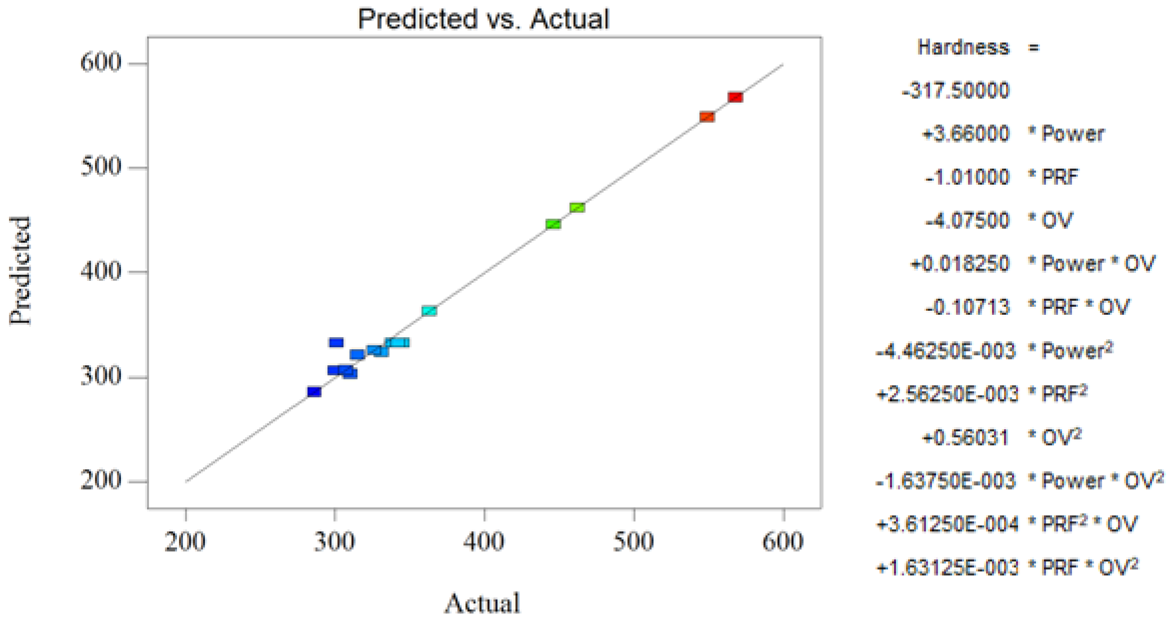

Figure 4 Plot of predicted data vs the actual data for the box Behnken experiment design for the samples processed with 20%Ar-80%Ni, and the equation for the model, using the model shown in Figure 2.

3.2 Microstructure

Figure 5 shows a comparison of the microstructure of 316L stainless steel pin samples laser processed using argon and 20% argon-80% nitrogen, respectively, with the parameters corresponding to sample 1 and 11 in Table 3. The altered region is indicated by 1, and the bulk substrate material by 2. Martensite phase microstructure can be seen in the altered region, which is not present in the austenitic un-altered region. The composition was measured by EDX. The EDX data for sample 6, which exhibited the highest microhardness, is presented in Figure 6, and the composition found is presented in Table 4. The table gives a nitrogen weight percentage of 1.41%. However it can be seen on the inset image in Figure 6 that there is no discernible nitrogen peak. Thus it can only be concluded that the nitrogen content is below the limit of detection. Surface back-scatter electron images showing a top-down view of the surface of samples processed with argon or the 20% argon 80% nitrogen mix can be seen in Figure 7. The bright material visible in the images is the hard martensite, and the dark material is the softer ferrite. The bright material was not visible for in the as-received sample material, as 316L SST is only austenite in structure. The bright martensite structure is visible in the processed samples, due to the melting and resolidification of the surface material. More of the bright material is visible in the sample processed with 20%Ar-80%Ni mixture than the sample processed with the pure argon.

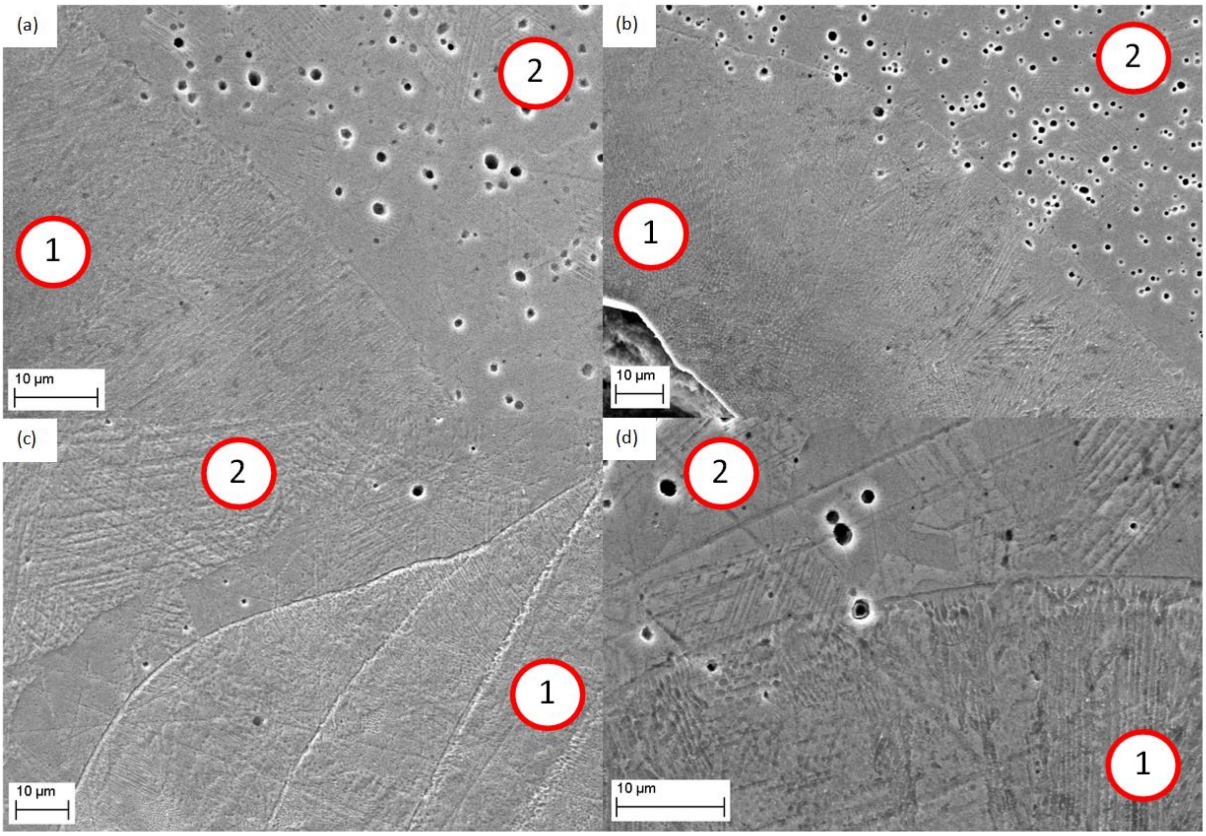

Figure 5 SEM cross-section micrographs of 316L samples (a) sample 1 processed with argon, (b) sample 1 processed with 20% argon 80% nitrogen, (c) sample 11 processed with argon, and (d) sample 11 processed with 20% argon 80% nitrogen.

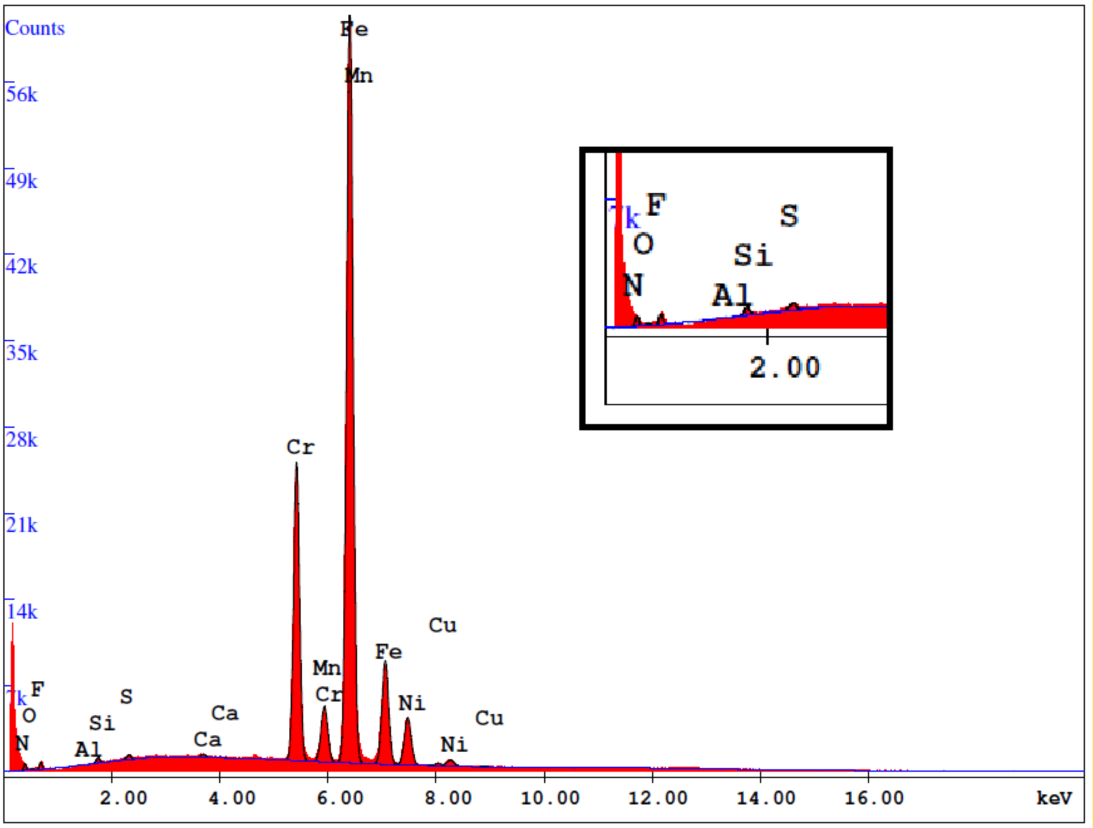

Figure 6 EDX plot for DoE sample 6, with inset showing a close up on the expected location of the nitrogen peak.

Table 4 Composition table from EDX plot shown in Figure 6.

Element	N	O	F	Al	Si	S	Ca	Cr	Mn	Fe	Ni	Cu
Weight %	1.41	0.14	0.68	0.00	0.41	0.24	0.13	17.01	1.61	70.97	7.01	0.40

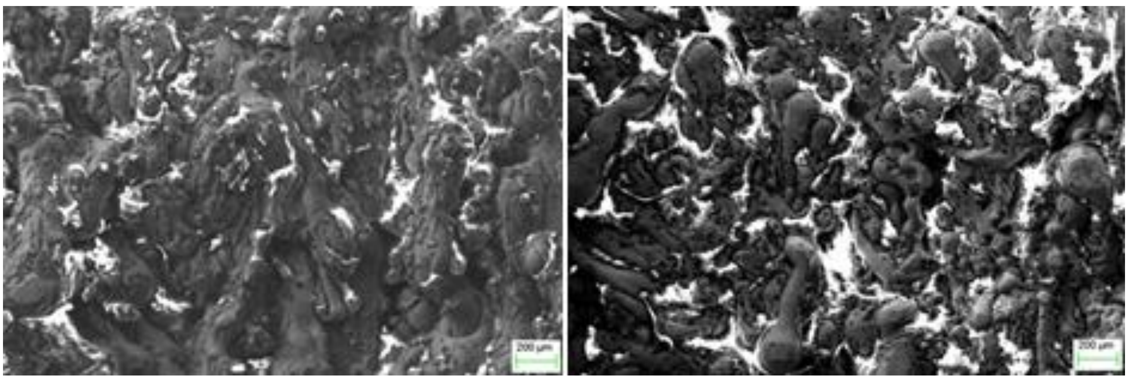

(a) (b)

Figure 7 Surface back-scatter electron images of the surface of stainless steel samples processed with (a) pure argon and (b) a 20% argon 80% nitrogen mix.

From the analysis of hardness test results, EDX, and the surface BSE images, it can be concluded that laser processing in nitrogen gas atmosphere boosts the formation of the hard martensite (the bright portion in the BSE image) compared to the soft ferrite (dark). The absorption of nitrogen by the metal surface is below the limits of detection in the EDX measurement. One factor affecting the nitrogen absorption is the low CO_2 laser photon energy of 0.12 eV, which is below the 15.6 eV required to ionise the nitrogen gas and the 9.8 eV required for the dissociation. The power density applied in this experiment was $1.2x10^6$ kW/cm^2 which is also small compared to the irradiation of $3x10^{10}$ kW/cm^2 needed for the gas breakdown. As such, this lowers the amount of nitrogen that can be absorbed into the molten metal, compared to methods using ionised nitrogen such as plasma nitriding or ion-beam nitriding. The difference in microstructure and hardness could be influenced by incorporation of nitrogen in amounts below the threshold for detection by EDX, however it seems more likely that the main mechanism is the increased cooling rates for nitrogen, compared to argon, leading to increased martensite formation.

3.3 Wear testing

Flat 316L stainless steel samples were laser processed to create a flat equivalent for sample 11 in Table 3, for pin-on-disc wear testing, using either argon or a 20%Ar-80%Ni mix. The results of the wear testing can be seen in Table 5. There was some improvement in the wear resistance by processing with argon, and a greater improvement processing with the argon nitrogen mixture.

Table 5 Wear behavior of 316L stainless steel without laser processing, and after laser processing with either only argon or the argon-nitrogen mixture.

Process gas	Mass Loss (g)	Reduction in Wear (%)
As-received	0.0203	-
Laser process with argon gas	0.0089	56.15
Laser process with 20%Ar-80%Ni mix	0.0007	96.55

The improvement can be explained by the increase in surface hardness, due to the harder martensite in the modified layer. The argon-nitrogen mixture performs better due to nitrogen's suppression of the formation of softer ferrite microstructure. Nitrogen is known to have higher thermal conductivity than argon [27], which allows it to achieve higher cooling rates during processing. Martensite microstructure is formed under rapid quenching [26], so laser processing with nitrogen will encourage the formation of hard martensite over the other softer microstructures. Figure 8 shows SEM images of the worn and un-worn surface for the samples processed with pure argon or an argon-nitrogen mixture. The wear track suggests an abrasive and adhesive wear mechanism that is the removed material smears the sample surface. The bright material visible in the images is the hard martensite, and the dark material is the softer ferrite. The bright material is not visible for the as-received sample material, and more of the bright material is visible in the sample processed with 20%Ar-80%Ni mixture than the sample processed with the pure argon. This supports this interpretation that the higher hardness and wear resistance is due to the harder microstructure.

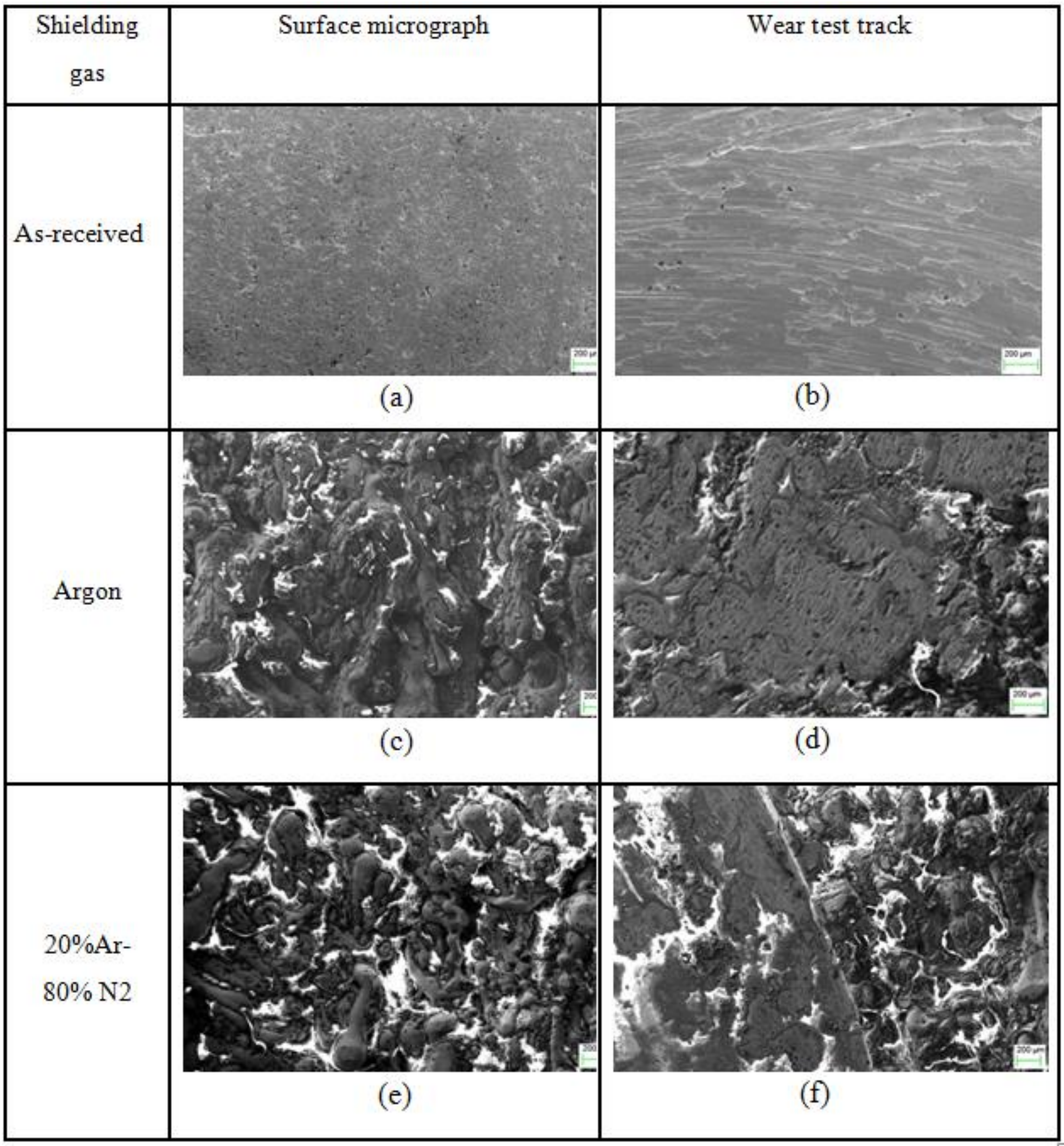

Figure 8 Surface of 316L SST flat samples (a) & (b) as received; (c) & (d) laser processed in argon; and (e) & (f) laser processed in argon-nitrogen mix.

4 Conclusion

In this work, laser surface treatment of 316L stainless steel, under a jet of either pure argon or a 20% argon 80% nitrogen mixture, was investigated. For the samples, which had an initial hardness of 250-280 HV, the highest hardness of 590 HV was achieved with the parameters of 400 W, 300 Hz, and 20% overlap using the 20%Ar-80%Ni mix. A strong direct proportionality between the pulse repetition frequency and the hardness was observed for the positive overlap. The material's hardness decreased with depth into the sample, but was significantly raised for (>500 HV) for over 400 μm. While plasma nitriding has previously been shown to achieved higher hardness results at the surface for 316L [25], the depth reported, ~7 μm, was significantly lower than the depths found in this work. For applications where parts are subject to wear eroding the surface, the depth of the treatment may be a more important factor than the highest hardness at the surface. The wear resistance of flat SST samples was seen to improve with processing, with greater improvement found from using the 20%Ar-80%Ni mix. The microstructure examination showed that a martensite phase had been created in an altered layer at the surface by the laser processing, with more present for the samples treated with the 20%Ar-80%Ni mix than the pure argon.

These results indicate that laser processing improves the hardness by creating a harder martensite microstructure in a layer at the surface, with the nitrogen creating a more martensite microstructure leading to the greater improvement in mechanical properties.

Acknowledgments

The authors would like to thank the funding agency Enterprise Ireland for funding this work under grant IP 2016 0517.

References

[1] Dutta Majumdar J, Nath a. K, Manna I. Studies on laser surface melting of tool steel — Part II: Mechanical properties of the surface. Surf Coatings Technol 2010;204:1326–9. doi:10.1016/j.surfcoat.2009.08.012.

[2] Chikarakara E, Naher S, Brabazon D. High speed laser surface modification of Ti–6Al–4V. Surf Coatings Technol 2012;206:3223–9. doi:10.1016/j.surfcoat.2012.01.010.

[3] Lavvafi H, Lewandowski ME, Schwam D, Lewandowski JJ. Effects of surface laser treatments on microstructure, tension, and fatigue behavior of AISI 316LVM biomedical wires. Mater Sci Eng A 2017;688:101–13. doi:10.1016/j.msea.2017.01.083.

[4] Aqida SN, Maurel M, Brabazon D, Naher S, Rosso M. Thermal stability of laser treated die material for semi-solid metal forming. Int J Mater Form 2009;2:761–4. doi:10.1007/s12289-009-0540-7.

[5] Schaaf P. Laser nitriding of metals. Prog Mater Sci 2002;47:1–16.

[6] Zhecheva A, Sha W, Malinov S, Long A. Enhancing the microstructure and properties of titanium alloys through nitriding and other surface engineering methods. Surf Coatings Technol 2005;200:2192–207. doi:10.1016/j.surfcoat.2004.07.115.

[7] Katayama S, Matsunawa A, Morimoto A, Ishimoto S, Arata Y. Surface hardening of titanium by laser nitriding. J Met 1983;35:85.

[8] Allmen M V., Blatter A. Laser-Beam Interactions with Materials. Volume 2. Springer Science & Business Media; 2013.

[9] Trtica MS, Tarasenko VF, Gaković BM, Fedenev A V., Petkovska LT, Radak BB, et

al. Surface modifications of TiN coating by pulsed TEA CO2 and XeCl lasers. Appl Surf Sci 2005;252:474–82. doi:10.1016/j.apsusc.2005.01.029.

[10] Yilbas BS, Karatas C, Ersu B, Gurgan S. Laser gas-assisted nitriding of Ti implant. Ind Lubr Tribol 2011;63:293–302.

[11] Sun F, Liu J, Yang Y, Yu H. Nitridation of iron by CW-CO2 laser nitriding technologies. Mater Sci Eng B Solid-State Mater Adv Technol 2005;122:29–33. doi:10.1016/j.mseb.2005.04.010.

[12] Mridha S, Baker TN. Crack-free hard surfaces produced by laser nitriding of commercial purity titanium. Mater Sci Eng A 1994;188:229–39. doi:10.1016/0921-5093(94)90376-X.

[13] Mordike B. Laser Surface Treatment of Metals. Springer; 1986.

[14] Morton P, Bell T, Weisheit A, Kroll J, Mordike B, Sagoo K. Laser gas nitriding of titanium and titanium alloys. In: Sudarshan T, Braza J, editors. Surf. Modif. Technol. V, Maney Publishing; 1992, p. 593–609.

[15] Bell T, Bergmann H, Lanagan J, Morton P, Staines A. Surface engineering of titanium with nitrogen. Surf Eng 2013.

[16] Grenier M, Dubé D, Adnot a., Fiset M. Microstructure and wear resistance of CP titanium laser alloyed with a mixture of reactive gases. Wear 1997;210:127–35. doi:10.1016/S0043-1648(97)00043-4.

[17] Selamat MS, Baker TN, Watson LM. Study of the surface layer formed by the laser processing of Ti-6Al-4V alloy in a dilute nitrogen environment. J Mater Process Technol 2001;113:509–15. doi:10.1016/S0924-0136(01)00595-7.

[18] Xin H, Watson LM, Baker TN. Surface analytical studies of a laser nitrided Ti ± 6Al ± 4V alloy : a comparison of spinning and stationary laser beam modes. Acta Metall 1998;46:1949–61.

[19] Wen J, Lundin CD. Surface Tension of 304 Stainless Steel under Welding Conditions. Weld J 1986;7:2226.

[20] Le M, Ville F, Kleber X, Cavoret J, Briancon L. Influence of Gas Nitriding on Rolling Contact Fatigue : Application on Alloyed Steels for Gears. Tribol Lubr Technol 2015;February:20–2.

[21] Ribeiro KJB, de Sousa RRM, de Araújo FO, de Brito RA, Barbosa JCP, Alves C. Industrial application of AISI 4340 steels treated in cathodic cage plasma nitriding technique. Mater Sci Eng A 2008;479:142–7. doi:10.1016/j.msea.2007.06.033.

[22] Lin K, Li X, Sun Y, Luo X, Dong H. Active screen plasma nitriding of 316 stainless steel for the application of bipolar plates in proton exchange membrane fuel cells. Int J Hydrogen Energy 2014;39:21470–9. doi:10.1016/j.ijhydene.2014.04.102.

[23] Ou K-L, Chou H-H, Liu C-M, Peng P-W. Surface modification of austenitic stainless steel with plasma nitriding for biomedical applications. Surf Coatings Technol 2011;206:1142–5. doi:10.1016/j.surfcoat.2011.08.001.

[24] Obeidi MA, McCarthy E, Brabazon D. Methodology of laser processing for precise control of surface micro-topology. Surf Coatings Technol 2016;307:702–12. doi:10.1016/j.surfcoat.2016.09.075.

[25] Biehler J, Hoche H, Oechsner M. Corrosion properties of polished and shot-peened austenitic stainless steel 304L and 316L with and without plasma nitriding. Surf Coatings Technol 2017;313:40–6. doi:10.1016/j.surfcoat.2017.01.050.

[26] Selvan JS, Subramanian K, Nath AK. Effect of laser surface hardening on En18 (AISI 5135) steel. J Mater Process Technol 1999;91:29–36. doi:10.1016/S0924-0136(98)00430-0.

[27] Lemmon EW, Jacobsen RT. Viscosity and thermal conductivity equations for nitrogen, oxygen, argon, and air. Int J Thermophys 2004;25:21–69. doi:10.1023/B:IJOT.0000022327.04529.f3.